

# Topological Spin Texture Created by Zhang–Rice Singlets in Cuprate Superconductors

Takao Morinari\*<sup>†</sup>

*Yukawa Institute for Theoretical Physics, Kyoto University, Kyoto 606-8502, Japan*

One of the most important effects of strong electron correlation in high- $T_c$  cuprates is the formation of Zhang–Rice singlets. By fully accounting for the quantum correlation effect of Zhang–Rice singlet formation, we show that a topological spin texture, *skyrmion*, is created around a Zhang–Rice singlet in the single-hole-doped  $\text{CuO}_2$  plane. The skyrmion picture provides a natural connection between the antiferromagnetic correlation and the doping concentration  $x$ .

KEYWORDS: high- $T_c$ , Zhang–Rice singlet, skyrmion,  $\text{CuO}_2$  plane, single-hole-doped system

## 1. Introduction

It has been over two decades since the discovery of hole-doped high-critical-temperature (high- $T_c$ ) superconductivity in copper oxides.<sup>1</sup> However, despite the many novel pictures presented, the mechanism behind the phenomenon remains elusive. One of the difficulties in explaining high- $T_c$  cuprates is the presence of a strong electron correlation, which is responsible for the Mott insulating state<sup>2</sup> in the parent undoped compound. Understanding this strong correlation in the doped Mott insulator would be the key to unveiling the mechanism behind the superconductivity.

The Mott insulating state of the parent compound is a type of charge-transfer insulator.<sup>3</sup> The basic electronic structure of the  $\text{CuO}_2$  plane, which is the key structure in high- $T_c$  cuprates, is described by the  $d$ – $p$  model.<sup>4</sup> An important observation was made by Zhang and Rice<sup>5</sup> about the description of a doped hole. Owing to the presence of a Cu–O hybridization term, there is a strong antiferromagnetic (AF) interaction  $J_K$  between an O  $p$ -hole and a Cu  $d$ -hole. When one considers combinations of four O-hole states around a Cu site, the symmetric state with respect to the Cu site interacts with the Cu spin through an enhanced AF interaction. This strong correlation leads to a singlet state—the so-called Zhang–Rice singlet.

---

<sup>†</sup>Present address: Graduate School of Human and Environmental Studies, Kyoto University, Kyoto 606-8501, Japan

\*E-mail address: morinari.takao.5s@kyoto-u.ac.jp

By restricting the Hilbert space where every doped hole forms a Zhang–Rice singlet and by excluding doubly occupied sites, the  $d$ - $p$  model is reduced to the single-band  $t$ - $J$  model, which has been studied extensively.<sup>6</sup>

The original analysis by Zhang and Rice was based on a small-cluster Hamiltonian consisting of a single Cu site and four surrounding O sites. However, if one takes a different point of view, the problem of describing Zhang–Rice singlet formation is equivalent to the problem of describing a singlet state in a Mott insulator. However, here, in contrast to that in the cluster analysis, many-body effects should be considered. This kind of problem is generally quite difficult. In fact, describing a singlet state in a metal has been one of the central problems in condensed-matter physics since its discovery.<sup>7,8</sup> In particular, a doped hole does not just form a Zhang–Rice singlet state, but has a certain amplitude of hopping to neighboring sites. Another nontrivial effect is that of the molecular fields created by nearest-neighbor Cu spins. In the presence of molecular fields, a singlet state changes from the pure singlet state to a state having a finite induced moment. In this study, we show that both of these effects play an important role in forming a topological spin texture, *skyrmion*, around a Zhang–Rice singlet. The physical picture that a skyrmion is formed around a Zhang–Rice singlet was proposed by the present author in ref. 9, and the mechanism of  $d_{x^2-y^2}$ -wave superconductivity based on skyrmions was proposed in ref. 10. However, the microscopic mechanism of forming a skyrmion has not been established yet. Here, we demonstrate that a skyrmion is formed around a Zhang–Rice singlet on the basis of a microscopic model for high- $T_c$  cuprates.

The skyrmion spin texture is a solution of the O(3) nonlinear  $\sigma$  model (NL $\sigma$ M).<sup>11</sup> The low-energy effective theory of the two-dimensional AF Heisenberg model is described by NL $\sigma$ M:<sup>12</sup>

$$S_{NL\sigma M} = \frac{1}{g} \int dx \int dy \int d(c_{sw}t) \left[ \frac{1}{c_{sw}^2} (\partial_t \mathbf{n})^2 - (\partial_x \mathbf{n})^2 - (\partial_y \mathbf{n})^2 \right]. \quad (1)$$

Here, the continuous unit-vector field  $\mathbf{n} = \mathbf{n}(\mathbf{r}, t)$  in a two-dimensional space  $\mathbf{r} = (x, y)$  represents the local direction of the Néel order parameter,  $c_{sw}$  is the spin-wave velocity, and  $g$  is the coupling constant. If we consider a static configuration of  $\mathbf{n}$ , the states can be classified into homotopy sectors<sup>13</sup> characterized by the topological charge

$$Q = \int dx \int dy \rho_{tc}(x, y), \quad (2)$$

with the topological charge density

$$\rho_{tc}(\mathbf{r}) = \frac{1}{8\pi} \mathbf{n} \cdot (\partial_x \mathbf{n} \times \partial_y \mathbf{n} - \partial_y \mathbf{n} \times \partial_x \mathbf{n}). \quad (3)$$

It is important to note that<sup>13</sup> any states in a given sector cannot move into another sector by

continuous deformation. The lowest energy in each sector is given by<sup>11</sup>

$$E_{NL\sigma M} = 4\pi|Q|. \quad (4)$$

The skyrmion is the lowest-energy state in the  $Q = 1$  sector. The explicit form is

$$\mathbf{n}_{sk}(\mathbf{r}, \lambda) = \left( \frac{2\lambda x}{r^2 + \lambda^2}, \frac{2\lambda y}{r^2 + \lambda^2}, \frac{r^2 - \lambda^2}{r^2 + \lambda^2} \right), \quad (5)$$

with  $r = \sqrt{x^2 + y^2}$  being the radial coordinate in space.

In the early days of high- $T_c$  research, a skyrmion spin texture was conjectured<sup>14</sup> to correspond to the spinon excitation in the resonating-valence-bond theory.<sup>15</sup> When a Hopf term is added to  $S_{NL\sigma M}$ , skyrmions can have fermionic statistics.<sup>16</sup> However, it was shown later that there is no Hopf term in the two-dimensional AF Heisenberg model.<sup>17–19</sup> Thus, the possibility of identifying a skyrmion with a spinon was ruled out.

Since a skyrmion is a metastable solution of  $NL\sigma M$ , there must be additional terms necessary to stabilize it. Such terms are inferred by scaling analysis where  $(x, y) \rightarrow (\alpha x, \alpha y)$ . One can see that the energy of the  $NL\sigma M$  is scale-invariant, which is consistent with the skyrmion energy being independent of  $\lambda$ . If there is a term that scales as  $1/\alpha$ , it is possible to have a stable skyrmion. For example, in the  $\nu = 1$  quantum Hall system, one finds that the long-range Coulomb interaction scales as  $1/\alpha$ . A skyrmion is stable provided that the Zeeman energy is sufficiently small.<sup>20</sup> In a doped antiferromagnet, Shraiman and Siggia pointed out<sup>21</sup> that the AF long-range order in the undoped system gives way to a non-collinear spiral state after hole doping. This spiral correlation is induced by a hole hopping term. The competition between the AF correlation and the spiral correlation leads to a modified hopping term that has an  $SU(2)$  matrix form in spin space. The components of the  $SU(2)$  matrix are determined by the spin configuration along the hopping direction.<sup>22</sup> In the continuum, one can see that this hopping term scales as  $1/\alpha$ . However, it turns out that just having this term is not sufficient to stabilize a skyrmion.

In this paper, we fully account for quantum effects in the formation of Zhang–Rice singlets in the single-hole-doped  $\text{CuO}_2$  plane to show that a skyrmion spin texture is formed around the singlet. The crucial point is that we need *both* the presence of a Zhang–Rice singlet and the hopping effect favoring a spiral state.

This paper is organized as follows. In §2, we introduce the model that describes the single-hole-doped  $\text{CuO}_2$  plane. In §3, we present the numerical diagonalization result that suggests that a half-skyrmion spin texture is formed around a Zhang–Rice singlet. In §4, we present the self-consistent skyrmion configuration. In §5, the physical consequences of the skyrmion

picture are discussed. Section 6 is devoted to the conclusion.

## 2. Model

We consider a doped hole in the  $\text{CuO}_2$  plane in a skyrmion spin texture background. In the single-hole-doped  $\text{CuO}_2$  plane, the system gains energy from Cu-O hybridization that leads to an AF interaction between O and Cu holes.<sup>5</sup> Zhang and Rice<sup>5</sup> considered the combinations of the four O-hole states around a Cu ion, and showed that the singlet state between a Cu hole and a symmetric O-hole state with respect to the central Cu ion has the largest binding energy. By projecting out the other O-hole states, the  $t$ - $J$  model was derived.<sup>5</sup> Although we assume that the correlation of forming this singlet state is the most important electronic correlation, we do not restrict ourselves to the Hilbert space where the singlet is fully formed. The Hamiltonian is

$$\begin{aligned} \mathcal{H} = & -t \sum_{\langle \ell, \ell' \rangle, \sigma} (p_{\ell' \sigma}^\dagger p_{\ell \sigma} + \text{h.c.}) + 2J_K \mathbf{S}_0 \cdot (\psi_0^\dagger \boldsymbol{\sigma} \psi_0) \\ & + \frac{J_K}{2} \sum_{j(\neq 0), \ell} \mathbf{S}_j \cdot (p_{\ell}^\dagger \boldsymbol{\sigma} p_{\ell}) + J \sum_{\langle i, j \rangle} \mathbf{S}_i \cdot \mathbf{S}_j, \end{aligned} \quad (6)$$

Here, the indices  $\ell$  and  $\ell'$  refer to O sites, and  $i$  and  $j$  refer to Cu sites. The hole hopping integral  $t$  is restricted to nearest-neighbor sites, and the components of  $\boldsymbol{\sigma} = (\sigma_x, \sigma_y, \sigma_z)$  are the Pauli matrices. The exchange interaction  $J$  between Cu spins  $\mathbf{S}_j$  is restricted to nearest-neighbor sites. The operator  $p_{\ell \sigma}^\dagger$  creates an O ( $2p_x, 2p_y$ ) hole with spin  $\sigma$  at site  $\ell$ . In order to describe Zhang–Rice singlet formation, the Cu spin at the center is described by the quantum spin

$$\mathbf{S}_0 = \frac{1}{2} (d_0^\dagger \boldsymbol{\sigma} d_0), \quad (7)$$

with  $d_0^\dagger = (d_{0\uparrow}^\dagger, d_{0\downarrow}^\dagger)$ . The operator  $d_{0\sigma}^\dagger$  creates a Cu  $3d_{x^2-y^2}$  hole with spin  $\sigma$  at the central Cu site. The second term of eq. (6) describes the interaction of forming a Zhang–Rice singlet. The operator  $\psi_0$  consists of four O-hole states around the quantum Cu spin at the center and is given by

$$\psi_{0\sigma} = \frac{1}{2} \sum_{\ell \in \{0\}} p_{\ell \sigma}. \quad (8)$$

If we take a strong  $J_K$  limit, the Zhang–Rice singlet is fully formed and eq. (6) is reduced to the  $t$ - $J$  model. However, here, we do not take this limit.

We assume a skyrmion configuration for  $\mathbf{S}_j$  except at the origin ( $j = 0$ ). By representing

the coordinate vector of the Cu site  $j$  by  $\mathbf{R}_j$ ,  $\mathbf{S}_j$  is given by

$$\mathbf{S}_j = (-1)^j S \mathbf{n}_{sk}(\mathbf{R}_j, \lambda), \quad (9)$$

where  $\mathbf{n}_{sk}$  is defined by eq. (5). For  $S$ , we set  $S = 1/2$ . (If we take into account the effect of quantum fluctuations,  $S$  is somewhat reduced. However, we neglect this for simplicity.) We use NL $\sigma$ M in evaluating the energy associated with the last term in eq. (6). The energy of a spin texture in NL $\sigma$ M is given by eq. (4). The salient feature of this energy formula is that the energy is independent of the skyrmion size  $\lambda$ . The resulting spin texture can be different from the originally assumed skyrmion configuration because of the presence of a quantum Cu spin at the origin. However, the static Cu spin configuration is still characterized by the topological charge  $Q$ , and the energy is given by eq. (4) as long as we consider the lowest energy state in the homotopy sector with  $Q$ . Since eq. (6) is independent of the skyrmion size  $\lambda$ , we may focus on the energy of the hole and the quantum spin  $\mathbf{S}_0$  and their interaction with other Cu spins. Therefore, the Hamiltonian eq. (6) is reduced to the following form:

$$\begin{aligned} \mathcal{H} = & -t \sum_{\langle \ell, \ell' \rangle, \sigma} (p_{\ell' \sigma}^\dagger p_{\ell \sigma} + \text{h.c.}) + J_K (d_0^\dagger \boldsymbol{\sigma} d_0) \cdot (\psi_0^\dagger \boldsymbol{\sigma} \psi_0) \\ & + \frac{J_K}{2} \sum_{j(\neq 0), \ell} \mathbf{S}_j \cdot (p_\ell^\dagger \boldsymbol{\sigma} p_\ell) + \frac{J}{2} \sum_{\langle 0, j \rangle} (d_0^\dagger \boldsymbol{\sigma} d_0) \cdot \mathbf{S}_j + E_{NL\sigma M}. \end{aligned} \quad (10)$$

In the second last term, we consider the interaction between  $\mathbf{S}_0$  and its nearest neighbor Cu spins. In the analysis below, we denote energies in units of  $t$ .

### 3. Skyrmion Creation around Zhang–Rice Singlet

The Hamiltonian eq. (10) is exactly diagonalized in the Hilbert space where each of the central Cu-hole and the O-hole states is singly occupied. For  $J$ , we assume  $J/t = 1/3$ , which is a standard value taken from the literature.<sup>6</sup> The  $\lambda$  dependence of the ground-state energy is shown in Fig. 1. The ground-state energy exhibits a clear energy minimum for  $J_K > 1$ . In particular, the minimum is located at  $\lambda \simeq a$ , and this value is insensitive to an increase in  $J_K$  for  $J_K > 1.5$ .

Now, we estimate  $J_K$ . From the second-order perturbation theory with respect to the Cu-O hybridization term,<sup>5</sup>  $J_K$  is given by

$$J_K = \frac{2t_{dp}^2}{U_d - \Delta} + \frac{2t_{dp}^2}{U_p + \Delta}, \quad (11)$$

where  $t_{dp}$  is the wave-function overlap of Cu and O holes.  $U_p$  is the on-site Coulomb repulsion at an O site and  $U_d$  is the on-site Coulomb repulsion at a Cu site. The parameter  $\Delta$  is given by  $\Delta = \varepsilon_p - \varepsilon_d$ , with  $\varepsilon_p$  and  $\varepsilon_d$  being the atomic energies of the O and Cu holes, respectively.

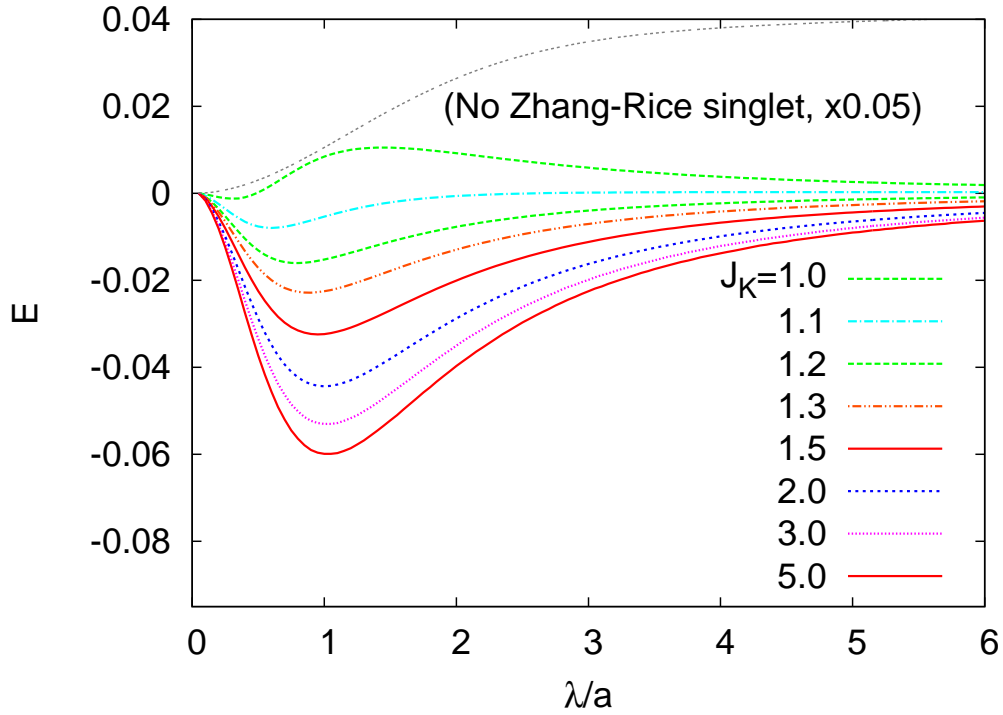


**Fig. 1.** (Color online) Skyrmion core size  $\lambda$  dependences of the ground-state energy of the doped hole Hamiltonian eq. (6) for different values of  $J_K$ . The energy without a Zhang–Rice singlet for  $J_K = 2$  is also shown. The energies are measured from their values at  $\lambda = 0$ . In describing the  $\text{CuO}_2$  plane, we employed a  $21 \times 21$  square lattice for Cu sites and a  $12 \times 12$  square lattice for O sites with open-boundary conditions.

Using the parameter set taken from constrained local density approximation calculations,<sup>23</sup> we find  $J_K \simeq 2$ . Therefore, a skyrmion with a core size of  $\lambda \simeq a$  is formed around the Zhang–Rice singlet. Since the core state is the Zhang–Rice singlet state, where there is no topological charge density, this result suggests that a *half-skyrmion* with  $|Q| = 1/2$  is created around the Zhang–Rice singlet. It is important to note that the presence of the Zhang–Rice singlet is crucial to stabilization of the skyrmion. Thus, if one replaces the quantum Cu spin with the classical spin, the minimum disappears, as shown in Fig. 1.

The location of the energy minimum at  $\lambda \simeq a$  can be explained by a simple calculation. Let us consider a cluster consisting of a single Cu site at  $(0, 0)$  and four surrounding O sites at  $(\pm a/2, 0)$ ,  $(0, \pm a/2)$ . We assume that there are molecular fields at the O sites created by other Cu spins at  $(\pm a, 0)$  and  $(0, \pm a)$ . Then, the exact diagonalization of this cluster Hamiltonian is carried out analytically. (The details of the calculation is presented in Appendix .) For the radial configuration of the molecular fields, which is equivalent to the skyrmion configuration

with  $\lambda = a$ , we find that the energy is given by

$$E_r = -\frac{3J_K + 2t}{2} - \frac{1}{2} \sqrt{(3J_K + 2t)^2 + S^2 J_K^2}. \quad (12)$$

Meanwhile, for the AF configuration of the molecular fields, we find

$$E_{AF} = -J_K - 2t - \sqrt{\left(2J - \frac{J_K}{2}\right)^2 S^2 + 4J_K^2}. \quad (13)$$

Using the parameters for the  $\text{CuO}_2$  plane, we find  $E_r < E_{AF}$  as shown in Fig. A-2. This can be simply understood as follows: In order to maximize the energy gain by creating the Zhang–Rice singlet state, the system prefers to have the molecular fields cancel each other. This is achieved for the radial configuration. By contrast, the molecular field effect is maximized for the AF configuration.

The instability of the homotopy sector with  $Q = 0$ , which corresponds to the AF state, is understood in the following way as well. In order to clarify the physical picture, we rewrite the NL $\sigma$ M by introducing complex fields  $z_\sigma(\mathbf{r}, t)$  through

$$\mathbf{n}(\mathbf{r}, t) = \sum_{\sigma, \sigma'=\uparrow, \downarrow} z_\sigma^*(\mathbf{r}, t) \boldsymbol{\sigma}_{\sigma, \sigma'} z_{\sigma'}(\mathbf{r}, t), \quad (14)$$

and we obtain the CP<sup>1</sup> model<sup>13</sup>

$$S_{CP^1} = \frac{4}{g} \int dx \int dy \int d(c_{sw}t) \sum_{\sigma=\uparrow, \downarrow} \left[ \left| \left( \frac{1}{c_{sw}} \partial_t - i\alpha_0 \right) z_\sigma(\mathbf{r}, t) \right|^2 - |(\partial_x + i\alpha_x) z_\sigma(\mathbf{r}, t)|^2 - |(\partial_y + i\alpha_y) z_\sigma(\mathbf{r}, t)|^2 \right], \quad (15)$$

with

$$\alpha_0 = i \sum_{\sigma=\uparrow, \downarrow} z_\sigma^*(\mathbf{r}, t) \frac{\partial}{\partial(c_{sw}t)} z_\sigma(\mathbf{r}, t), \quad (16)$$

$$\boldsymbol{\alpha} = \frac{i}{2} \sum_{\sigma=\uparrow, \downarrow} \{ z_\sigma^*(\mathbf{r}, t) \nabla z_\sigma(\mathbf{r}, t) - [\nabla z_\sigma^*(\mathbf{r}, t)] z_\sigma(\mathbf{r}, t) \}. \quad (17)$$

The equation of motion for the steady state is given by

$$(\nabla + i\boldsymbol{\alpha})^2 z_\sigma = 0. \quad (18)$$

In the presence of the Zhang–Rice singlet, the boundary condition at the origin is

$$z_\sigma(0) = 0. \quad (19)$$

In the AF configuration, there is no gauge flux,  $\nabla \times \boldsymbol{\alpha} = 0$ . Therefore, the equation of motion is reduced to

$$\nabla^2 z_\sigma = 0. \quad (20)$$

Using the polar coordinate  $r$  and  $\phi$  with  $x = r \cos \phi$  and  $y = r \sin \phi$ , let  $z_\sigma = f_\sigma(r) \exp(i\ell\phi)$ . Here,  $\ell$  is an integer. The equation for  $f_\sigma(r)$  is given by

$$\frac{d^2 f_\sigma}{dr^2} + \frac{1}{r} \frac{df_\sigma}{dr} - \frac{\ell^2}{r^2} f_\sigma = 0. \quad (21)$$

To be consistent with the assumption that there is no gauge flux, we must take  $\ell = 0$ . The equation is readily solved and we find

$$f_\sigma \propto \ln r. \quad (22)$$

Clearly, this solution is incompatible with the boundary condition eq. (19).

In the case that there is a nonvanishing gauge flux, it is difficult to solve the equation of motion because it is a nonlinear equation with respect to  $z_\sigma(\mathbf{r}, t)$ . However, it is possible to find the behavior of the solution near  $r = 0$ . If we assume  $z_\sigma = f_\sigma(r) \exp(i\ell\phi)$  with  $\ell \neq 0$ , we find

$$\boldsymbol{\alpha} = -\frac{\ell}{r} \sum_\sigma f_\sigma^2 \mathbf{e}_\phi, \quad (23)$$

where  $\mathbf{e}_\phi = (-\sin \phi, \cos \phi)$ . From eq. (18), after some algebra, we obtain

$$\frac{d^2 f_\sigma}{dr^2} + \frac{1}{r} \frac{df_\sigma}{dr} - \frac{\ell^2}{r^2} \sum_\sigma (1 - f_\sigma^2)^2 f_\sigma = 0. \quad (24)$$

For  $r \rightarrow 0$ , the solution of this equation behaves as

$$f_\sigma \rightarrow C_\sigma r^{|\ell|}, \quad (25)$$

with  $C_\sigma$  as a constant. Note that this form is consistent with the boundary condition eq. (19). Since  $\ell \neq 0$ , there is a gauge flux. The situation is quite similar to the problem of the point singularity in a two-dimensional superfluid.<sup>24</sup> The vortex in  $z_\sigma(\mathbf{r})$  turns out to be a skyrmion. In fact the topological charge density eq. (3) is expressed as

$$\rho_{tc}(\mathbf{r}) = -\frac{1}{2\pi} (\partial_x \alpha_y - \partial_y \alpha_x), \quad (26)$$

in terms of the gauge flux.<sup>13</sup> Therefore, a nonvanishing gauge flux is a skyrmion characterized by the topological charge eq. (2).

#### 4. Self-Consistent Skyrmion Configuration

In the previous section, we have presented the numerical result that suggests that a half-skyrmion spin texture is formed around the Zhang–Rice singlet. In this calculation, Cu spins except that at the origin are assumed to be a skyrmion spin texture given by eq. (9). In this section, we attempt to obtain the self-consistent spin configuration by fixing the directions of the four Cu spins surrounding the Zhang–Rice singlet.



The self-consistent Cu spin configuration is obtained by solving the mean field equations. At each Cu site, there are molecular fields created by the nearest-neighbor Cu sites and O-hole. In the self-consistent configuration, the Cu spin at each site is antiparallel to this molecular field. To describe the  $\text{CuO}_2$  plane, we employ a  $15 \times 15$  square lattice for Cu sites and a  $10 \times 10$  square lattice for O sites under the open-boundary condition. As explained below, the doped hole is strongly localized around the Zhang–Rice singlet. Therefore, a large system is not necessary in describing doped hole hopping. According to the energy calculation in Fig. 1 and the cluster analysis above, we fix the four Cu spins around the center. As shown in the self-consistent spin configurations in Fig. 2, the difference between the skyrmion and the anti-skyrmion is only that the  $x$ -components of the spins are reversed. Furthermore, as shown in Fig. 2(c), the doped hole is strongly localized around the quantum Cu spin. In the absence of the Zhang–Rice singlet, the doped hole is not localized but extended. Therefore, the formation of a skyrmion is not sufficient to localize the doped hole.

The physically important quantity is the topological charge density shown in Fig. 2(d). Note that rotation of all spins about the  $z$ -axis through the same angle does not change the topological character. However, the topological charge changes sign for the anti-skyrmion case. It is important to note that the topological charge density is considerably extended when compared with the doped hole wave function. Since the topological charge distribution produces a magnetic-field-like effect through the Berry phase,<sup>25</sup> the non-vanishing topological charge density carried by the doped hole produces intriguing effects, as will be discussed below. The sum of the topological charge is 0.320, whereas the expected value is one-half. This discrepancy is probably associated with the approximation in describing Cu spins by classical spins. In fact, the calculation above overestimates the AF correlation that reduces the total topological charge. Describing Cu spins using more suitable fields is a future problem.

The existence of a stable skyrmion spin texture in a Li-doped system was suggested by Haas *et al.*<sup>26</sup> in the  $t - J$  model with one hole on a 13-site cluster. In the cluster, the central Cu site is replaced by Li. The exact diagonalization of the cluster system under the boundary condition imposed by the skyrmion configuration shows that the total energy has a minimum at  $\lambda \simeq 2a$ . In their calculation, the doped hole cannot reside at the center site and is bounded by the attractive Coulomb potential of Li. Although the system is not equivalent to our system, the mechanism of stabilizing a skyrmion is quite similar. In the model in ref. 26, the doped hole is localized owing to the attractive Coulomb potential. In our system, however, the doped hole is localized by the formation of the Zhang–Rice singlet. The stability of a skyrmion is also demonstrated in a 16-site cluster<sup>27</sup> with hole motion being restricted to four sites around

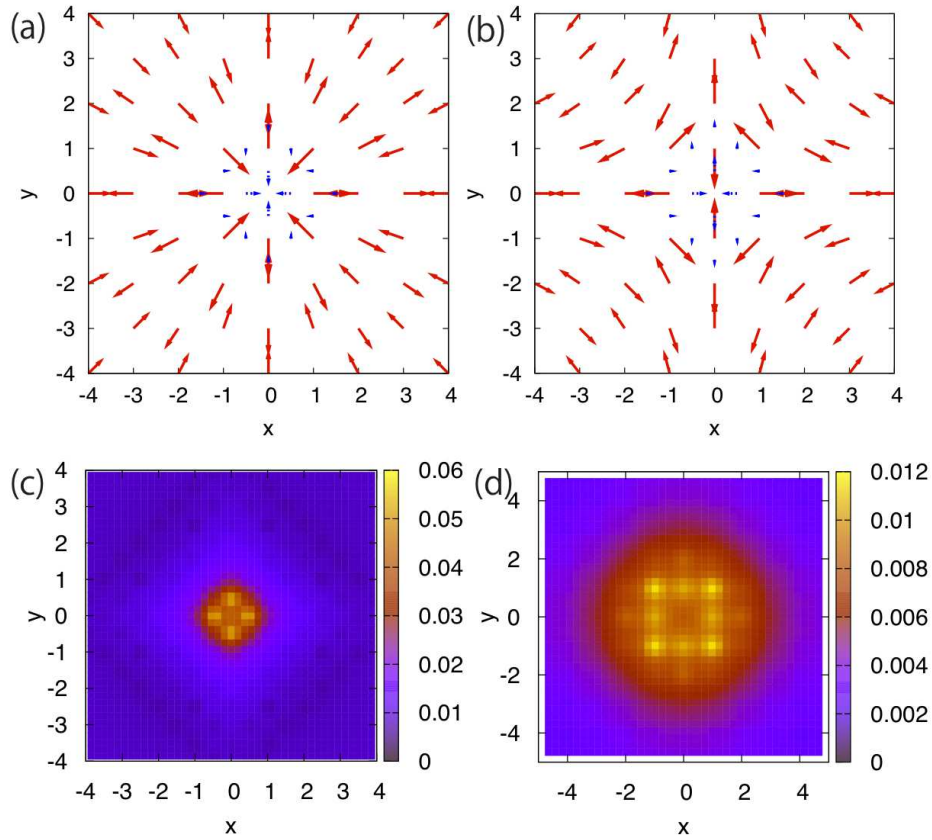


**Fig. 2.** (Color online) Self-consistent Cu spin configuration in the case of a skyrmion (a) and an anti-skyrmion (b). The dashed arrows represent the doped hole spin, which is scaled by a factor of 10. (c) Doped hole density and (d) topological charge density for the skyrmion (a).

the center.

## 5. Discussion

Now, we explore the physical consequences of the skyrmion spin texture created by a doped hole. The most direct consequence is that the magnetic properties are straightforwardly connected with the hole doping concentration  $x$ . As revealed by neutron scattering measurements,<sup>28</sup> the inverse of the AF correlation length  $\xi_{AF}$  is well described by the simple formula

$$\kappa(x, T) = \kappa(x, 0) + \kappa(0, T), \quad (27)$$

where  $T$  is the temperature. The inverse of the temperature-independent term  $\kappa(x, 0)$  is given by

$$\frac{1}{\kappa(x, 0)} = \frac{a}{\sqrt{x}}. \quad (28)$$

The right-hand side of this equation is the average separation between the doped holes. Meanwhile,  $\kappa(0, T)$  is described by the formula for  $NL\sigma M$ .<sup>29</sup> The latter is associated with the underlying AF correlation. When each doped hole creates a skyrmion, local spin disorder is created by the skyrmion. Therefore, the average hole separation leads to a temperature-independent component of  $\xi_{AF}$ . Another important observation is that the skyrmion character is lost at approximately around  $x \sim 0.3$ , where the average hole separation is  $\sim 2a$ . In the vicinity of this critical doping level, each doped hole is unable to create a skyrmion with  $\lambda = a$  and so all skyrmion features are lost for  $x > 0.3$ .

As we have seen above, the doped hole is localized by the formation of the Zhang–Rice singlet. Therefore, Nagaoka ferromagnetism<sup>30</sup> does not occur and the system is insulating in a slightly doped regime. The energy band of doped holes forms when the overlap of adjacent doped hole wave functions is not negligible. The bandwidth  $W$  is proportional to the wave function overlap.

As mentioned above, the presence of a skyrmion leads to a Berry phase effect. The skyrmion produces a magnetic-field-like effect for doped holes. When a doped hole enters a region of skyrmion spin texture created by another doped hole, then the Lorentz force effectively acts between the two holes. This interaction leads to a chiral pairing state.<sup>10</sup> Since there are skyrmions and anti-skyrmions, two chiral pairing states coexist with opposite chiralities. The analysis of the gap equation suggests that this type of interaction leads to  $d_{x^2-y^2}$ -wave superconductivity.<sup>10,31</sup>

In addition, skyrmion dynamics has a nontrivial contribution to hole dynamics. The skyrmion itself has its own dynamics, which is not identical to bare hole dynamics.<sup>9</sup> The doped hole moves with a constraint of keeping the skyrmion as long as  $W < J$ . The underlying Fermi surface, which appears when the skyrmion is suppressed, is partially gapped because the skyrmion energy does not necessarily vanish along it, which results in a truncated Fermi surface.<sup>31</sup> For this pseudogap phenomenon, the characteristic temperature is the binding energy of the skyrmion, which is  $\sim 0.04t$  from Fig. 1. The order of magnitude for this value is the same as that of the pseudogap temperature evaluated in materials with high  $T_c$  cuprates.<sup>32</sup> However, for elaborate investigations of the pseudogap, a better description is necessary. In this regard, it is worth pointing out that the Hamiltonian describing the dynamics of the composite object comprising the doped hole and skyrmion is similar to that for quasiparticles in the  $d$ -density wave state.<sup>33</sup> However, the physical picture is quite different.

Here, we comment on electron-doped high- $T_c$  cuprates. The superconducting state of electron-doped cuprates has a  $d$ -wave pairing symmetry,<sup>34</sup> which is the same as that in the

hole-doped case. From this observation one might expect that the mechanisms of superconductivities are the same for electron-doped and hole-doped cuprates. However, the superconducting transition temperature of electron-doped cuprates is quite low compared with that of hole-doped cuprates with high transition temperatures. Furthermore, there are qualitative differences between electron-doped and hole-doped cuprates. Among others, the relationships between superconductivity and antiferromagnetism are strikingly different. In hole-doped cuprates, only 2 – 3% hole doping is sufficient to kill AF order, while we need about 20% electron doping to suppress AF order in electron-doped cuprates. In the phase diagram in the plane of doping concentration and temperature, the superconducting phase is clearly separated from the AF phase in hole-doped cuprates, while the superconducting phase and the AF phase sit side by side in the electron-doped cuprates.<sup>35</sup> Therefore, it is quite natural to surmise a different mechanism for superconductivity works in electron-doped cuprates. If the mechanism is different, it is quite hard to describe such a difference in the single-band Hubbard model. Meanwhile, the difference is simply associated with the presence or absence of skyrmions in the skyrmion picture. In electron-doped cuprates, Zhang-Rice singlets are irrelevant because electron carriers are introduced at Cu sites and there is no singlet correlation between electron carriers and Cu *d*-electrons. Therefore, a skyrmion is not formed in electron-doped cuprates.

Finally, we propose a “smoking-gun” experiment to establish the presence of skyrmions in high- $T_c$  cuprates. In the doping range of  $0.02 < x < 0.055$ , incommensurate inelastic magnetic peaks are observed in neutron-scattering experiments.<sup>36,37</sup> In the skyrmion picture, these peaks are associated with the AF skyrmion lattice.<sup>31</sup> Recently, real-space observations of a two-dimensional skyrmion lattice have been reported in  $\text{Fe}_{0.5}\text{Co}_{0.5}\text{Si}$ .<sup>38</sup> This experimental technique can be applied to finding the skyrmion lattice in high- $T_c$  cuprates as well.

## 6. Conclusions

To conclude, we have shown that a skyrmion spin texture is created around a Zhang–Rice singlet in the single-hole-doped  $\text{CuO}_2$  plane. The evolution of the AF correlation upon hole doping is naturally described by the skyrmion picture. A doped hole with a skyrmion creates the Berry phase effect, which can lead to *d*-wave superconductivity. The skyrmion picture also seems to be consistent with some other aspects of high- $T_c$  cuprates.

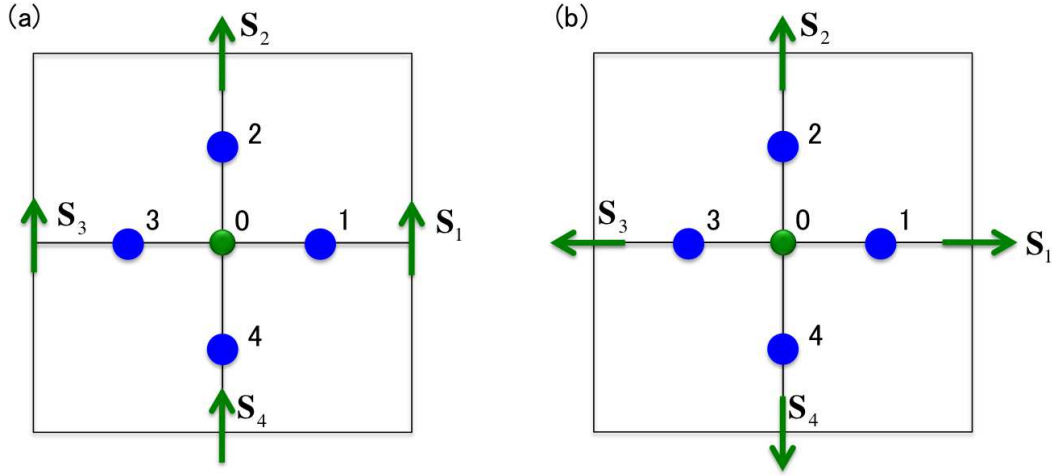


**Fig. A-1.** (Color online) Molecular fields  $\mathbf{S}_j$  ( $j = 1, 2, 3, 4$ ) at Cu sites for the (a) AF configuration and (b) radial configuration. The circle at the center denotes the quantum Cu spin. The O sites are labeled as 1, 2, 3, and 4.

## Acknowledgments

I would like to thank S. Brazovski, N. Nakai, and L. Cai for discussions and T. Tohyama for comments. This work was supported by a Grant-in-Aid for the Global COE Program “The Next Generation of Physics, Spun from Universality and Emergence” from the Ministry of Education, Culture, Sports, Science and Technology (MEXT) of Japan.

## Appendix: Derivation of Eqs. (12) and (13)

In this Appendix, we present the derivation of eqs. (12) and (13). We consider a cluster that consists of one quantum Cu spin sitting at the center, four O sites, and four classical Cu spins  $\mathbf{S}_j$ , as shown in Fig. A-1. For convenience, we introduce the following field:

$$\gamma_{q\sigma} = \frac{1}{2} \sum_{\ell=1,2,3,4} \exp(iq(\ell-1)) p_{\ell\sigma}, \quad (\text{A}\cdot 1)$$

where  $q = 0, \pi/2, \pi, 3\pi/2$ . In terms of these fields, the Hamiltonian of the cluster is given by

$$\begin{aligned} \mathcal{H} = & 2t \sum_{\sigma} \left( -\gamma_{0\sigma}^{\dagger} \gamma_{0\sigma} + \gamma_{\pi\sigma}^{\dagger} \gamma_{\pi\sigma} \right) + J_K \left( d_0^{\dagger} \sigma d_0 \right) \cdot \left( \gamma_0^{\dagger} \sigma \gamma_0 \right) \\ & + \frac{J_K}{2} \sum_{j,p,q} \left( M_j \right)_{pq} \mathbf{S}_j \cdot \left( \gamma_p^{\dagger} \sigma \gamma_q \right) + \frac{J}{2} \sum_j \mathbf{S}_j \cdot \left( d_0^{\dagger} \sigma d_0 \right), \end{aligned} \quad (\text{A}\cdot 2)$$

where  $(M_j)_{pq} = (U^\dagger)_{pj}U_{jq}$  with

$$U = \frac{1}{2} \begin{pmatrix} 1 & 1 & 1 & 1 \\ i & -i & 1 & -1 \\ -1 & -1 & 1 & 1 \\ -i & i & 1 & -1 \end{pmatrix}. \quad (\text{A}\cdot 3)$$

For the AF configuration of  $\mathbf{S}_j$  (Fig. A·1(a)), we take  $\mathbf{S}_j = S\mathbf{e}_z$ , where  $\mathbf{e}_z$  is the unit vector in the  $z$ -direction. The third term in eq. (A·2) has the following simple form:

$$\frac{SJ_K}{2} \sum_p \gamma_p^\dagger \sigma_z \gamma_p. \quad (\text{A}\cdot 4)$$

In the Hilbert space, where each of the central Cu states and O states is singly occupied, the Hamiltonian is diagonalized analytically, and we find that the ground-state energy is given by eq. (13).

For the radial configuration of  $\mathbf{S}_j$  [Fig. A·1(b)], we take  $\mathbf{S}_1 = S\mathbf{e}_x$ ,  $\mathbf{S}_2 = S\mathbf{e}_y$ ,  $\mathbf{S}_3 = -S\mathbf{e}_x$ , and  $\mathbf{S}_4 = -S\mathbf{e}_y$ . Here,  $\mathbf{e}_x$  and  $\mathbf{e}_y$  are the unit vectors in the  $x$ - and  $y$ -directions, respectively. In this case, the third term in eq. (A·2) has the form

$$\frac{SJ_K}{2} \left( \gamma_{\pi/2}^\dagger \sigma_- \gamma_0 + \gamma_{-\pi/2}^\dagger \sigma_+ \gamma_0 + \gamma_0^\dagger \sigma_+ \gamma_{\pi/2} + \gamma_0^\dagger \sigma_- \gamma_{-\pi/2} \right), \quad (\text{A}\cdot 5)$$

where  $\sigma_\pm = (\sigma_x \pm i\sigma_y)/2$ . Noting that this term does not contain  $\gamma_{\pi\sigma}$  or  $\gamma_{\pi\sigma}^\dagger$ , we find that the Hilbert space is divided into subspaces. Explicitly considering spin states of the Cu spin state and the O hole state, the problem is reduced to diagonalize the following  $4 \times 4$  matrix:

$$\begin{pmatrix} -2t - J_K & 2J_K & \frac{SJ_K}{2} & 0 \\ 2J_K & -2t - J_K & 0 & \frac{SJ_K}{2} \\ \frac{SJ_K}{2} & 0 & 0 & 0 \\ 0 & \frac{SJ_K}{2} & 0 & 0 \end{pmatrix}. \quad (\text{A}\cdot 6)$$

By taking the lowest eigenenergy of this reduced Hamiltonian, we obtain eq. (12).

The energies of eqs. (12) and (13) are shown in Fig. A·2 as functions of  $S$ . Here, we assume  $J_K/t = 2$  and  $J/t = 1/3$ . In the entire range of  $S$ , the energy of eq. (12) is lower than the energy of eq. (13). We find that  $E_r < E_{AF}$  for  $J_K/t > 0.66$ . For  $J_K/t < 0.66$ ,  $E_r > E_{AF}$  in the entire range of  $S$ .

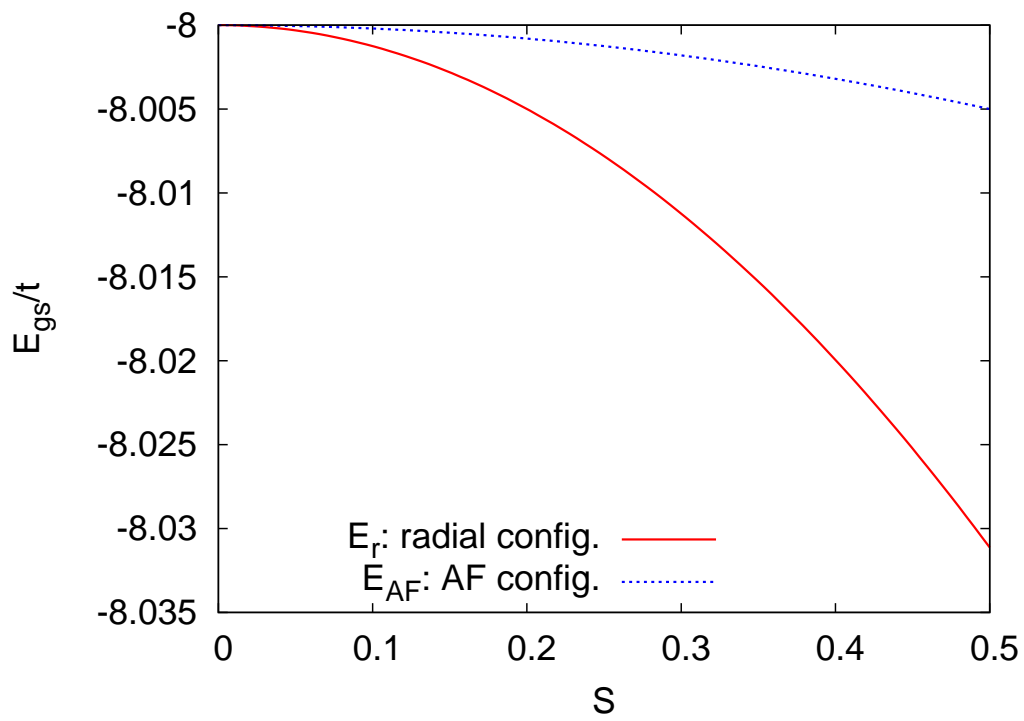


**Fig. A-2.** (Color online)  $E_r$  and  $E_{AF}$  as functions of the spin  $S$  for  $J_K/t = 2$ .

**References**

- 1) J. G. Bednorz and K. A. Müller: *Z. Phys. B: Condens. Matter* **64** (1986) 189.
- 2) M. Imada, A. Fujimori, and Y. Tokura: *Rev. Mod. Phys.* **70** (1998) 1039.
- 3) J. Zaanen, G. A. Sawatzky, and J. W. Allen: *Phys. Rev. Lett.* **55** (1985) 418.
- 4) V. J. Emery: *Phys. Rev. Lett.* **58** (1987) 2794.
- 5) F. C. Zhang and T. M. Rice: *Phys. Rev. B* **37** (1988) 3759.
- 6) P. A. Lee, N. Nagaosa, and X. G. Wen: *Rev. Mod. Phys.* **78** (2006) 17.
- 7) J. Kondo: *Prog. Theor. Phys.* **32** (1964) 37.
- 8) A. Hewson: *The Kondo problem to heavy fermions* (Cambridge Univ Press, New York, 1997).
- 9) T. Morinari: *Phys. Rev. B* **72** (2005) 104502.
- 10) T. Morinari: *Phys. Rev. B* **73** (2006) 064504.
- 11) A. A. Belavin and A. M. Polyakov: *JETP Lett.* **22** (1975) 245.
- 12) S. Chakravarty, B. I. Halperin, and D. R. Nelson: *Phys. Rev. B* **39** (1989) 2344.
- 13) R. Rajaraman: *Solitons and instantons* (North-Holland, New York, 1987).
- 14) I. Dzyaloshinskii, A. Polyakov, and P. Wiegmann: *Phys. Lett. A* **127** (1988) 112.
- 15) P. W. Anderson: *Science* **235** (1987) 1196.
- 16) F. Wilczek and A. Zee: *Phys. Rev. Lett.* **51** (1983) 2250.
- 17) F. D. M. Haldane: *Phys. Rev. Lett.* **61** (1988) 1029.
- 18) E. Fradkin and M. Stone: *Phys. Rev. B* **38** (1988) 7215.
- 19) X. G. Wen and A. Zee: *Phys. Rev. Lett.* **61** (1988) 1025.
- 20) S. L. Sondhi, A. Karlhede, S. A. Kivelson, and E. H. Rezayi: *Phys. Rev. B* **47** (1993) 16419.
- 21) B. I. Shraiman and E. D. Siggia: *Phys. Rev. Lett.* **62** (1989) 1564.
- 22) V. Korenman, J. L. Murray, and R. E. Prange: *Phys. Rev. B* **16** (1977) 4032.
- 23) M. S. Hybertsen, M. Schlüter, and N. E. Christensen: *Phys. Rev. B* **39** (1989) 9028.
- 24) A. Fetter and J. Walecka: *Quantum Theory of Many-Particle Systems* (Courier Dover Publications, New York, 2003).
- 25) M. V. Berry: *Proc. R. Soc. A* **392** (1984) 45.



- 26) S. Haas, F.-C. Zhang, F. Mila, and T. M. Rice: Phys. Rev. Lett. **77** (1996) 3021.
- 27) R. J. Gooding: Phys. Rev. Lett. **66** (1991) 2266.
- 28) B. Keimer, N. Belk, R. J. Birgeneau, A. Cassanho, C. Y. Chen, M. Greven, M. A. Kastner, A. Aharony, Y. Endoh, R. W. Erwin, and G. Shirane: Phys. Rev. B **46** (1992) 14034.
- 29) P. Hasenfratz and F. Niedermayer: Phys. Lett. B **268** (1991) 231 .
- 30) Y. Nagaoka: Phys. Rev. **147** (1966) 392.
- 31) T. Morinari: in *The Multifaceted Skrymion*, eds. G. E. Brown and M. Rho (World Scientific, Singapore, 2010) Chap. 13, p. 311.
- 32) T. Timusk and B. W. Statt: Rep. Prog. Phys. **62** (1999) 61.
- 33) S. Chakravarty, R. B. Laughlin, D. K. Morr, and C. Nayak: Phys. Rev. B **63** (2001) 094503.
- 34) C. C. Tsuei and J. R. Kirtley: Phys. Rev. Lett. **85** (2000) 182.
- 35) A. Damascelli, Z. Hussain, and Z. X. Shen: Rev. Mod. Phys. **75** (2003) 473.
- 36) S.-W. Cheong, G. Aeppli, T. E. Mason, H. Mook, S. M. Hayden, P. C. Canfield, Z. Fisk, K. N. Clausen, and J. L. Martinez: Phys. Rev. Lett. **67** (1991) 1791.
- 37) K. Yamada, C. H. Lee, K. Kurahashi, J. Wada, S. Wakimoto, S. Ueki, H. Kimura, Y. Endoh, S. Hosoya, G. Shirane, R. J. Birgeneau, M. Greven, M. A. Kastner, and Y. J. Kim: Phys. Rev. B **57** (1998) 6165.
- 38) X. Yu, Y. Onose, N. Kanazawa, J. Park, J. Han, Y. Matsui, N. Nagaosa, and Y. Tokura: Nature **465** (2010) 901.